Long-range parity-nonconserving electron-nucleon interaction

V. A. Dzuba●, V. V. Flambaum●, and P. Munro-Laylim

School of Physics, University of New South Wales, Sydney 2052, Australia

As known, electron vacuum polarization by nuclear Coulomb field produces a Uehling potential with the range $\hbar/2m_e c$. Similarly, neutrino vacuum polarization by Z boson field produces long-range potential $\sim G^2/r^5$ with the large range $\hbar/2m_\nu c$. Attempts to measure the parity-conserving part of this potential produced only limits on this potential which are several orders of magnitude higher than the standard model predictions. We show that the parity nonconserving (PNC) part of the neutrino exchange potential $W_L(r)$ gives a significant fraction of the observed PNC effects. Mixed $Z - \gamma$ electron vacuum polarization produces a PNC potential with range $\hbar/2m_e c$, which exceeds the range of the weak interaction by five orders of magnitude. We calculate the contribution of the long-range PNC potentials to the nuclear spin-independent and nuclear spin-dependent PNC effects. The cases of the single-isotope PNC effects and the ratio of PNC effects in different isotopes are considered for Ca, Cs, Ba, Sm, Dy, Yb, Hg, Tl, Pb, Bi, Fr, Ra atoms and ions. Contributions of the long-range PNC potentials ($\sim 1\%$) significantly exceed the experimental error (0.35%) for PNC effect in Cs. The difference between potentials produced by Dirac neutrino and Majorana neutrino may, in principle, help to determine what kind of neutrino is realized in nature.

I. INTRODUCTION

As noted by Feynman [1] and calculated in Refs. [2–4], exchange by two neutrinos [see, e.g., the diagram in Fig. 1(a)] produces long-range potential $\sim G^2/r^5$, where G is Fermi constant. However, effects of the parity-conserving part of this potential are many orders of magnitude smaller than the sensitivity of experiments in Refs. [5–10].

In Ref. [11], it was noted that the neutrino exchange potential has a parity nonconserving (PNC) part. Earlier it was demonstrated that mixed $Z - \gamma$ electron vacuum polarization produces a PNC potential with the range $\hbar/2m_e c$ [see Fig. 1(b)], which exceeds the range of the weak interaction by five orders of magnitude [12]. In the present paper, we show that the contributions of the long-range PNC potentials to PNC effects in atoms is $\sim 1\%$ and this significantly exceeds the error 0.35% of the PNC measurement in the Cs atom [13] and the error <0.5% in the many-body atomic calculations of the Z-boson contribution [14–21]. Work is in progress to improve both experimental [22–24] and theoretical [25] accuracy.

The error in atomic calculations cancels out in the ratio of the PNC amplitudes in different isotopes of the same atom [26–28]. Work is in progress for such measurements too, in particular, for the chain of isotopes of a Yb atom [29]. The study of the PNC in atoms plays an important role in testing the standard model and searching for new physics beyond it [30,31].

Radiative corrections to the PNC amplitudes of the order $\alpha \approx 1/137$ have been presented as the radiative corrections to proton and neutron weak charges and exceed 1% [32]. Weak charge itself is the constant of the electron-nucleon

weak interaction due to the Z-boson exchange, which has interaction range $r_Z = \hbar/M_Z c = 0.002$ fm. On the nuclear and atomic scales, this may be considered a Fermi-type contact interaction. However, radiative corrections actually generate PNC interaction of a much longer range. Neutrino vacuum polarization by the nuclear weak Z boson field [see Fig. 1(a)] produces PNC potential $W_L(r) \propto 1/r^5$, which has exponential cutoff on the distance $r_\nu = \hbar/2m_\nu c$ exceeding atomic size by many orders of magnitude. Mixed $Z - \gamma$ electron vacuum polarization [see Fig. 1(b)] induces PNC interaction $\propto 1/r^3$ of the range $r_e = \hbar/2m_e c = 193$ fm [12], similar to the range of the Uehling potential due to electron vacuum polarization by the nuclear Coulomb field.

The deviation from the contact limit for this long-range PNC interaction may be significant since in heavy atoms relativistic Dirac electron wave functions rapidly increase toward the nucleus ($\psi_{s_{1/2}} \psi_{p_{1/2}} \propto 1/r^{2-2\gamma}$, where Z is the nuclear charge, $\gamma = \sqrt{1 - Z^2\alpha^2}$, so $2 - 2\gamma \approx Z^2\alpha^2$). This rapid variation of the electron wave function between $r_e = \hbar/2m_e c$ and the nucleus requires proper treatment of the long-range PNC potential W_L. Contrary to the contact PNC interaction W_Q, potential W_L gives a direct contribution to the matrix elements between electron orbitals with angular momentum higher than $l = 0$ and $l = 1$. Note that in Yb, the PNC mixing between dominating configurations is given by the $\langle p|W|d\rangle$ matrix element. Therefore, this qualitative feature of the long-range PNC interaction also should be investigated.

Note that deviation of the contribution of the long-range potential W_L from its contact interaction limit is roughly proportional to $\alpha(Z\alpha)^2$. Indeed, in the nonrelativistic limit ($Z\alpha \ll 1$), an s-wave function and gradient of a p-wave function are approximately constant near the nucleus and the PNC matrix
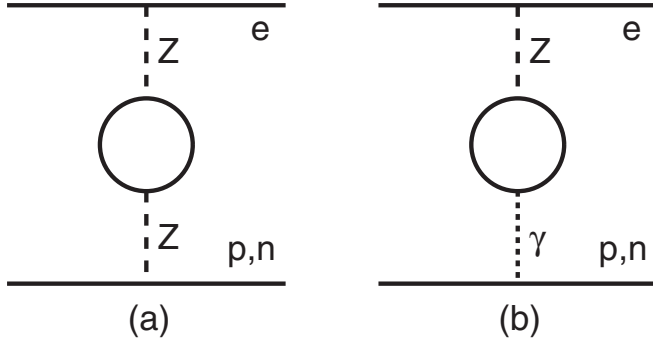
FIG. 1. (a) Vacuum polarization by the nuclear weak Z-boson field which produces long-range parity violating potential $W_L(r) \propto 1/r^5$. In the case of neutrino loop the range is $r_\nu = \hbar/2m_\nu c$. (b) Mixed $Z - \gamma$ vacuum polarization which produces long-range parity violating potential $W_L(r) \propto 1/r^3$. In the case of electron loop, the range is $r_e = \hbar/2m_e c$.

element $\langle s|W_L|p \rangle$ is not sensitive to the range of the potential as soon it is much smaller than a_B/Z. Other contributions of the order $\alpha(Z\alpha)$ may be found in Ref. [18] and references therein.

Note that the electron-positron loop may be replaced by the particle-hole pair corresponding to the excitation of electron from the atomic core. However, this is a correction which has already been included in the many-body calculations of the PNC effects. A different mechanism of the long-range PNC interaction between an atom and charged particle (via PNC vector polarizability) has been discussed in Ref. [33].

In the present paper, we consider corrections due to long-range PNC interaction to the PNC amplitudes in many atoms of experimental interest. We consider the cases of single isotope measurements and the ratio of the PNC amplitudes for a chain of isotopes. We perform calculations of the nuclear spin independent (NSI) interaction and the nuclear spin dependent (NSD) interaction. We also discuss the difference between the potentials produced by Dirac and Majorana neutrinos.

II. LONG-RANGE PNC POTENTIAL DUE TO THE MIXED PHOTON: Z VACUUM POLARIZATION

It was suggested in Ref. [12] that photon-Z-boson mixing via electron loop [see Fig. 1(b)] leads to the long-range PNC potential. In Ref. [12], this potential was obtained for a pointlike nucleus and contact Fermi-type interaction. The latter leads to a singular potential $W_L \propto 1/r^3$ and logarithmic divergency of the matrix elements for the interaction between electron and quark at $r \to 0$. To allow for a more accurate numerical calculations, we present this potential for the finite size R of the nucleus and cutoff for large momenta (small distances r) produced by the Z-boson propagator ($1/(q^2 + M_Z^2)$ instead of $1/M_Z^2$). The full PNC operator has the form

$$W(r) = \frac{G}{2\sqrt{2}} \gamma_5 \Bigg[-Q_W \rho(r), \tag{1}$$

$$+ \int d^3r' \rho(\mathbf{r}') \frac{2Z\alpha q m^2 c^2}{3\pi^2 \hbar^2} \frac{I(|\mathbf{r} - \mathbf{r}'|)}{|\mathbf{r} - \mathbf{r}'|} \Bigg], \tag{2}$$

$$\equiv W_Q(r) + W_L(r). \tag{3}$$

Here the first line presents contact PNC interaction $W_Q(r)$ and the second line is the long-range PNC interaction $W_L(r)$, $Q_W \approx -0.9884N + 0.07096Z$ [34] is the weak nuclear charge, $\rho(r)$ is the nuclear density normalised by condition $\int \rho(r)dV = 1$, α is the fine structure constant, and m is the mass of the fermion in the loop. In Eq. (2), the factor $q = (1 - 4\sin^2\theta_W)$ for electron and other charged leptons (μ, τ) of mass m. Quarks also contribute to the potential. For the u, c, t quarks, we have factor $3q = 2(1 - \frac{8}{3}\sin^2\theta_W)$; for the d, s, b quarks, the factor is $3q = (1 - \frac{4}{3}\sin^2\theta_W)$. These factors are the products of the electric and weak quark charges. They also include a factor of 3 for three possible quark colors. To reproduce proton weak charge $q_p = (1 - 4\sin^2\theta_W) = 0.07096$, including radiative corrections, we use a value of the Weinberg angle near the Z pole, $\sin^2\theta_W \approx 0.232$ (formally at zero momentum transfer $\sin^2\theta_W \approx 0.239$) [34]. Function $I(r)$ in Eq. (2) is given by

$$I(r) = \int_1^\infty \exp(-2xmcr/\hbar)\left(1 + \frac{1}{2x^2}\right)\frac{\sqrt{x^2 - 1}z^2 dx}{x^2 + z^2}, \tag{4}$$

where $z = M_Z/2m$. Note that this result takes into account that there is no $Z - \gamma$ mixing for zero momentum transfer. Function $I(r)/r$ gives us dependence of interaction between electron and quark on distance r between them. For large r, the function $I(r)/r \propto \exp(-2mcr/\hbar)/r^{5/2}$, for $\hbar/M_Z c \ll r \ll \hbar/mc$, we obtain $I(r)/r \approx \hbar^2/(4m^2c^2r^3)$ and this behavior gives logarithmic divergency of the matrix elements integrated with d^3r. Natural cutoff happens on $r \ll \hbar/M_Z c$, where $I(r)/r \propto (\ln r)/r$ and has no divergency integrated with d^3r. The interval $\hbar/M_Z c < r < \hbar/mc$ gives the dominating contribution to the matrix element since it is enhanced by the large parameter $\ln[M_Z/m]$.

PNC amplitudes are proportional to the matrix elements $\langle s_{1/2}|W_Q + W_L|p_{1/2}\rangle$. Let us start from the approximate analytical calculation of the ratio of the matrix elements of W_L and W_Q. Due to the singular behavior of $I(|\mathbf{r} - \mathbf{r}'|)/|\mathbf{r} - \mathbf{r}'|$ at small distance $|\mathbf{r} - \mathbf{r}'|$ between electron and quark inside the nucleus, we can replace $I(r)/r$ by its contact limit, $I(r)/r \to C\delta(\mathbf{r})$, where $C = \int (I(r)/r)d^3r$. After this substitution, operators W_L and W_Q are proportional to each other and we obtain the following result:

$$\frac{\langle ns_{1/2}|W_L|np_{1/2}\rangle}{\langle ns_{1/2}|W_Q|np_{1/2}\rangle} \approx \frac{W_L}{W_Q} \approx -\frac{2\alpha Z S}{3\pi Q_W}, \tag{5}$$

where

$$S = \sum_i q_i L_i$$

$$L_i = \left(1 - \frac{1}{2z_i^2}\right)\left(1 + \frac{1}{z_i^2}\right)^{1/2} \ln\left[z_i + \left(1 + z_i^2\right)^{1/2}\right]$$

$$- \frac{5}{6} + \frac{1}{2z_i^2} \approx \ln[M_Z/m_i] - \frac{5}{6},$$

where $z_i = M_Z/2m_i \gg 1$. Note that corrections to the last equality are very small, $\sim 1/z_i^2$. The result has a relatively weak logarithmic sensitivity to masses m_i. To have correct

exponential cutoff of the potential $W_L(r)$ at large distance, we should select quark mass which provides correct minimal hadron energy for the system containing quark-antiquark pair. In the case of u and d quarks, this is a pair of pions. Therefore, we select $2m_u = 2m_d = 2m_\pi = 280$ MeV, the minimal mass of hadrons in the loop in the diagram in Fig. 1(b). Similarly, we choose $2m_s = 2m_K = 987$ MeV (note that in the calculations of the radiative corrections to the weak charge, Ref. [32] used $2m_u = 2m_d = 2m_s \approx 200$ MeV). For heavy quark masses, we use their bare values $m_c = 1270$ MeV, $m_b = 4500$ MeV.

Ratio $Q_W/Z = -0.9884N/Z + 0.07096$ is approximately the same for all heavy atoms. Numerical estimate of expression Eq. (5) gives a correction to PNC amplitude of about 2%. If we consider the electron loop contribution only, we obtain the correction to PNC amplitude of 0.1%.

We have tested an analytical result in Eq. (5), obtained in the contact interaction approximation, by the accurate numerical calculations of the ratio of the matrix elements of W_Q and W_L. Our special interest is in deviation of the accurate result from the contact limit in Eq. (5). Zero approximation has been calculated using Hatree-Fock-Dirac relativistic electron wave functions. We perform the calculation of the core polarization effect using the random phase approximation. Correlation corrections have been included using the correlation potential method [35].

The effect of W_Q is proportional to the $\langle s_{1/2}|W_Q|p_{1/2}\rangle$ matrix elements. Other matrix elements are negligible in the Hartree-Fock approximation and gain significant values only due to the core polarization corrections, which are due to the $\langle s_{1/2}|W_Q|p_{1/2}\rangle$ weak matrix elements between the core and excited states. Contrary to the contact PNC interaction W_Q, the long-range interaction W_L gives a direct contribution to the matrix elements between electron orbitals with angular momentum higher than $l = 0$ and $l = 1$. However, the core polarization contribution still strongly dominates in such matrix elements. For example, in $\langle 6p_{3/2}|W_L|5d_{3/2}\rangle$ matrix element in the Cs atom, the core polarization contribution is 1000 times bigger than the direct contribution. For Ra$^+$, it is 470 times bigger. Therefore, the ratio of the W_L and W_Q contributions to the PNC effects is very close to the ratio of $s_{1/2} - p_{1/2}$ weak matrix elements. Note also that it is sufficient to calculate the ratio $\langle ns_{1/2}|W_L|np_{1/2}\rangle/\langle ns_{1/2}|W_Q|np_{1/2}\rangle$ for any principal quantum number n. This is because the values of these matrix elements come from short distances where the wave functions for different n differ by normalization only. The normalization cancels out in the ratio. We use lowest valence states in the calculations. The ratio is also the same for atoms and singly charged ions of these atoms.

The results of calculations for atoms and ions of experimental interest are presented in Table I in a form of the ratio of the (1) and (2) parts of the PNC operator, $\langle ns|W_L|np\rangle/\langle ns|W_Q|np\rangle$. We consider two cases, A and B. In case A, only the electron loop contribution to the long-range PNC potential Eq. (2) is included. In case B, contributions from all leptons (e μ, τ) and u, d, s, c, b quarks (except for t) are included. The reason for separating the electron contribution comes from the fact that this is the only true long-range contribution. The distances which give significant contributions to the matrix elements are much larger than

TABLE I. Ratios of PNC matrix elements $\langle ns|W_L|np\rangle/\langle ns|W_Q|np\rangle$ for atoms and singly charged ions of these atoms calculated in the contact approximation Eq. (5) and using accurate relativistic many-body theory. Numbers in square brackets mean powers of 10.

Atom	A[a]	A_c[b]	$(A-A_c)/A$	B[c]
^{40}Ca	1.33[−3]	1.37[−3]	−3.17%	2.84[−2]
^{85}Rb	9.69[−4]	1.04[−3]	−6.93%	2.15[−2]
^{133}Cs	8.42[−4]	9.43[−4]	−11.99%	1.96[−2]
^{135}Ba	8.46[−4]	9.49[−4]	−12.17%	1.97[−2]
^{149}Sm	8.37[−4]	9.54[−4]	−14.02%	1.98[−2]
^{163}Dy	7.88[−4]	9.09[−4]	−15.25%	1.88[−2]
^{171}Yb	7.96[−4]	9.26[−4]	−16.32%	1.92[−2]
^{199}Hg	7.54[−4]	8.97[−4]	−19.01%	1.86[−2]
^{203}Tl	7.42[−4]	8.85[−4]	−19.37%	1.84[−2]
^{207}Pb	7.31[−4]	8.74[−4]	−19.59%	1.81[−2]
^{209}Bi	7.33[−4]	8.78[−4]	−19.87%	1.82[−2]
^{213}Fr	7.62[−4]	9.23[−4]	−21.09%	1.92[−2]
^{223}Ra	7.16[−4]	8.69[−4]	−21.28%	1.80[−2]

[a]Electron loop contribution only.
[b]Contact approximation for A.
[c]Sum of the contributions from e, μ, τ, u, d, s, c, b. The numerical calculation results are very close to that given by formula Eq. (5).

the nuclear radius. The ranges of other contributions are still much bigger than the range of the weak interaction equal to the Z-boson Compton wavelength. However, their range is smaller than the nuclear radius and numerically the contributions of μ, τ, u, d, s, c, b may be described very accurately by the contact interaction.

III. RATIO OF PNC EFFECTS IN DIFFERENT ISOTOPES

It was suggested in Ref. [26] to measure the ratio of PNC amplitudes in different isotopes of the same atom. It was argued that electronic structure factor cancels out in the ratio and interpretation of the measurements does not require very difficult atomic calculations which have poor accuracy in atoms with more than one electron in open shells. In fact, the cancellation is not exact and corrections due to the change of the nuclear shape were considered in Refs. [27,28]. These include the change of the nuclear charge radius and neutron skin corrections. Here we consider one more correction to the ratio which comes from the long-range PNC potential. We have for the ratio of the PNC amplitudes in isotopes 1 and 2

$$\frac{A_{PNC1}}{A_{PNC2}} = \frac{\langle ns_{1/2}|W|np_{1/2}\rangle_1}{\langle ns_{1/2}|W|np_{1/2}\rangle_2}, \quad (6)$$

i.e., it is sufficient to study the ratio of the weak matrix elements. Let us introduce short notations, $\langle ns_{1/2}|W|np_{1/2}\rangle = Q_W K + K_L = Q_W K(1 + K_{LK}/Q_W)$. Here K is the electronic structure factor for the first term in Eq. (3), K_L is the matrix element of the long-range PNC potential, $K_{LK} = K_L/K$. Thus, the relative correction to the single isotope matrix element, presented in Eq. (5), here is denoted by K_{LK}/Q_W. Then the

ratio (6) becomes

$$\frac{A_{\text{PNC1}}}{A_{\text{PNC2}}} = \frac{Q_{W1}K_1 + K_{L,1}}{Q_{W2}K_2 + K_{L,2}} = \frac{K_1}{K_2} \frac{Q_{W1} + K_{LK,1}}{Q_{W2} + K_{LK,2}}. \quad (7)$$

It is important that $K_{LK} = K_L/K$ practically does not depend on the isotope, while Q_W is approximately proportional to the number of neutrons N, so dependence of Q_W on the isotope is significant. The relative difference of the PNC amplitudes for different isotopes may be approximately presented as

$$\frac{\Delta A}{A} \approx \left(\frac{\Delta A}{A}\right)_0 (1 - K_{LK}/Q_W), \quad (8)$$

where $A \equiv A_{\text{PNC}}$, $\Delta A = A_1 - A_2$, index 0 indicates the relative difference of the PNC amplitudes without long-range PNC interaction. Thus, the correction is equal to $-K_{LK}/Q_W$, so it has an sign to the single isotope correction K_{LK}/Q_W presented in Eq. (5) and Table I.

IV. LONG-RANGE NUCLEAR SPIN DEPENDENT PNC POTENTIAL

If we swap Z and γ in Fig. 1(b), we obtain a long-range PNC potential which depends on nuclear spin. Sum of the NSD PNC interaction mediated by the Z exchange [36] and NSD long-range PNC potential may be presented in the following form:

$$W(r) = \frac{G}{2\sqrt{2}} \gamma_0 (\boldsymbol{\Sigma}\boldsymbol{\gamma}) \Bigg[(1 - 4\sin^2\theta_W)\rho(r) \quad (9)$$

$$- \int d^3 r' \rho(\mathbf{r}') \frac{2\alpha q m^2 c^2}{3\pi^2 \hbar^2} \frac{I(|\mathbf{r} - \mathbf{r}'|)}{|\mathbf{r} - \mathbf{r}'|} \Bigg], \quad (10)$$

where $\Sigma = 1.27\langle \sum_n \sigma_n - \sum_p \sigma_p \rangle$. The result for the ratio of the long-range contribution to the Z-boson contribution differs from NSI PNC by the numerical factor $-Q_W/[Z(1 - 4\sin^2\theta_W)]$. This factor is approximately the same for all heavy atoms. For Cs, this factor is 18.5 and using Table I we obtain the electron loop contribution 1.55%. In the contact interaction limit, it is 13% bigger (for Fr and Ra$^+$ it is 21% bigger). Sum of the contributions from e, μ, τ, u, d, s, c, b loops increases the Z-boson contribution to the NSD PNC effects by 36%. Here the difference with the contact limit is small.

Note that we do not consider here NSD PNC interaction produced by the nuclear anapole moment [37,38] and the combination of the weak charge and hyperfine interaction [39].

V. LONG-RANGE PARITY NONCONSERVING POTENTIAL DUE TO EXCHANGE BY TWO NEUTRINOS

Exchange by two (nearly) massless neutrinos gives a long-range potential proportional to $1/r^5$. The parity-conserving part of this potential has been calculated in Refs. [2–4]. In addition to the diagram in Fig. 1(a), the electron neutrino contribution contains diagrams involving a W boson. Using their approach, we have found the PNC part of this $1/r^5$ potential ($\hbar = c = 1$):

$$W_\nu^{\text{PNC}}(r) = -\frac{G^2}{16\pi^3 r^5} Q_W (2 - N_{\text{eff}}) \gamma_5, \quad (11)$$

where N_{eff} is the effective number of the particles with the Compton wavelength larger than r. For the molecular scale, this is the number of neutrinos, $N_{\text{eff}} = 3$. However, the matrix element of this interaction in atoms converges at very small distances where ν, e, μ, τ, u, d, s, c, b contribute, giving $N_{\text{eff}} = 14.6$ (for the parity conserving part of the potential calculation of N_{eff} has been done in Ref. [10]). The potential Eq. (11) is very singular at small r and gives divergent matrix elements. To extend this potential to small distances, we present it for the finite size R of the nucleus and cutoff for large momenta (small distances r) produced by the Z-boson propagator ($1/(q^2 + M_Z^2)$ instead of $1/M_Z^2$). The full PNC operator has the form ($\hbar = c = 1$):

$$W(r) = -\frac{G}{2\sqrt{2}} Q_W \gamma_5 \Bigg[\rho(r) + (2 - N_{\text{eff}})$$

$$\times \frac{\sqrt{2}Gm^4}{3\pi^3} \int d^3 r' \rho(\mathbf{r}') \frac{I_2(|\mathbf{r} - \mathbf{r}'|)}{|\mathbf{r} - \mathbf{r}'|} \Bigg], \quad (12)$$

$$\equiv W_Q(r) + W_\nu^{\text{PNC}}(r). \quad (13)$$

For zero nuclear size and $\hbar/M_Z c \ll r \ll \hbar/mc$, Eq. (12) reproduces Eq. (11) if

$$I_2(r) = \int_1^\infty \exp(-2xmcr/\hbar)\left(x^2 - \frac{1}{4}\right) \frac{\sqrt{x^2 - 1}z^4 dx}{(x^2 + z^2)^2}, \quad (14)$$

where $z = M_Z/2m$. Function $I_2(r)/r$ gives us dependence of interaction between electron and quark on distance r between them. For large r, the function $I_2(r)/r \propto \exp(-2mcr/\hbar)/r^{5/2}$, for $\hbar/M_Z c \ll r \ll \hbar/mc$ we obtain $I_2(r)/r \propto 1/r^5$ and this behavior gives divergency $1/r_c^2$ of the matrix elements integrated with $d^3 r$. However, in the area $r \ll r_c = \hbar/M_Z c$ function $I_2(r)/r \propto (\ln r)/r$ and has no divergency integrated with $d^3 r$.

Note that the behavior of the neutrino exchange potential at small distance has been investigated in Ref. [40]. However, they do not study this potential in the standard model. They replaced the Z boson by some new scalar particle and studied the parity conserving potential only.

Convergence of the integral in the matrix elements $\langle s_{1/2}|W_\nu^{\text{PNC}}|p_{1/2}\rangle$ on the distance $r \sim r_c = \hbar/M_Z c$ indicates that this interaction in atoms may be treated as a contact interaction. Due to the singular behavior of W_L at small distance $|\mathbf{r} - \mathbf{r}'|$ between electron and quark inside the nucleus, we can replace $I_2(r)/r$ by its contact limit, $I_2(r)/r \to C\delta(\mathbf{r})$, where $C = \int (I_2(r)/r)d^3 r$. After calculation of the contact limit of $I_2(r)/r$, we obtain potential $W_\nu^{\text{PNC}}(r)$, which is proportional to the weak interaction mediated by the Z boson in Eq. (1). Therefore, we may present the result for the relative correction to the PNC amplitude as

$$\frac{W_\nu^{\text{PNC}}(r)}{W_Q(r)} = -\frac{GM_Z^2}{12\sqrt{2}\pi^2}(N_{\text{eff}} - 2) = -0.72\%, \quad (15)$$

This estimate of the $W_\nu^{\text{PNC}}(r)$ contribution significantly exceeds the experimental error of 0.35% for the Cs PNC amplitude. However, we may assume that a greater part of this correction has already been included among radiative corrections to the weak charge Q_W.

In Ref. [41], the parity-conserving potential has been obtained for a Majorana neutrino loop instead of a Dirac neutrino loop. Based on this result we conclude that PNC potential for

Majorana neutrinos contains

$$I_2^{(M)}(r) = \int_1^\infty \exp(-2xmcr/\hbar)\frac{(x^2-1)^{3/2}z^4 dx}{(x^2+z^2)^2}. \quad (16)$$

Replacement of the Dirac neutrino by a Majorana neutrino does not change the potential at small distance; the difference is proportional to $(m_\nu cr/\hbar)^2$ and is very small, the correction in the contact interaction limit is $\sim(m_\nu/M_Z)^2$. However, asymptotic expression at large distance changes, $I_2^{(M)}(r)/r \propto \exp(-2mcr/\hbar)/r^{7/2}$ [instead of $I_2(r)/r \propto \exp(-2mcr/\hbar)/r^{5/2}$ for the Dirac neutrino], so the ratio of the Dirac potential to the Majorana potential $\sim m_\nu cr/\hbar$ [41].

Calculation of the hadron loop contributions in Figs. 1(a) and 1(b) could, in principle, be refined using dispersive analysis of e^+e^- annihilation data. One can find examples of such an approach in calculations of radiative corrections to muon and electron magnetic moments and energy shifts in simple systems like muonium, positronium, and hydrogen—see, e.g., Ref. [42] and references therein. However, our case looks significantly different. The photon interacts with the vector fermion current while the Z boson interacts with both vector and axial currents, therefore, the result for the diagram in Fig. 1(a) can not be directly expressed in terms of experimental data for e^+e^- annihilation to hadrons, which goes mainly via intermediate photon. Reference [42] calculates numbers (corrections to magnetic moments and energy shifts) while, to recover the difference with the contact limit, we need to calculate functions $W_L(r)$. Reference [42] deals with simple systems while we perform calculations in heavy many-electron atoms with extended nucleus. Therefore, important aspects of the problem include relativistic many-body atomic theory. Finally, we do not aim here for $\sim1\%$ accuracy in the calculation of the hadron contribution, which is needed in the problem of the disagreement between theory and measurement of muon magnetic moment. Since the contribution of u and d quarks to the matrix elements of the potentials $W_L(r)$ does not exceed 50% and sensitivity to the input masses of these quarks is very weak, the dispersive analysis should not dramatically change our results. We leave this possible improvement for future study.

VI. DISCUSSION AND CONCLUSIONS

We calculated the long-range PNC potentials described by the diagram in Figs. 1(a) ($\propto1/r^5$) and 1(b) ($\propto1/r^3$). These potentials contribute to the PNC effects in atoms and molecules. Contrary to the contact weak interaction, these potentials may mix opposite parity orbitals with orbital angular momentum higher than $l=0$ and $l=1$, but $s_{1/2}$-$p_{1/2}$ mixing still gives a dominating contribution. Contribution of the $1/r^3$ potential in Fig. 1(b) to the NSI PNC effects is 2%, the contribution to the NSD effects is 40% of the Z-boson contribution. However, similar Feynman diagrams have already been included as the radiative corrections to the weak charge Q_W which is the source of the contact PNC interaction in atoms and molecules. Therefore, we may assume that only deviation from the contact approximation is an additional contribution to PNC effects. The diagram in Fig. 1(b) with the electron loop gives the PNC interaction range which exceeds the weak interaction

range due to Z-boson exchange $M_Z/2m_e = 10^5$ times. However, the electron loop contribution is only 0.1% of the weak charge Q_W contribution. For NSD PNC interaction, the electron loop contribution is 2% of the Z-boson contribution. Contributions of other charged fermions to the PNC matrix elements are very close to the contact limit since the range of corresponding interactions is smaller than the nuclear size.

Integrals in the matrix elements of the $1/r^5$ potentials are dominated by very small r and the corresponding interaction is accurately presented by its contact limit. Therefore, its effects may be treated as the radiative corrections to the weak charge Q_W and κ_2, which are the strength constants of the contact NSI and NSD weak interactions.

In Ref. [10], the parity-conserving part of the potential $1/r^5$ has been considered and compared with experimental data on muonium, positronium, hydrogen, and deuterium spectra and isotope shifts in hydrogen and calcium isotopes. The results have been expressed as limits on the interaction constant denoted as $G_{\rm eff}$ (this means that in the standard model formulas for energy shifts, the Fermi constant G has been replaced by $G_{\rm eff}$). These limits on $G_{\rm eff}$ are several orders of magnitude weaker than the tandard model predictions (including ν, e, μ, τ, u, d, s, c, b particles in the loop in the diagram in Fig. 1(a), from $G_{\rm eff}^2/G^2 < 4.0 \cdot 10^{11}$ to $G_{eff}^2/G^2 < 1.9 \times 10^2$. The latter limit is 18 orders of magnitude better than the limits obtained from macroscopic experiments in Refs. [5–10].

The situation with the PNC parts of the long-range potentials considered in the present paper is more optimistic. If following Ref. [10], we treat the interaction constant as a phenomenological parameter; then, from the Cs PNC experiment, we obtain $G_{\rm eff}^2 < 0.3G^2$ for the $1/r^3$ potential and $G_{\rm eff}^2 < G^2$ for the $1/r^5$ potential (theoretical and experimental errors have been added in quadrature).

Note that the potentials are different for Dirac and Majorana neutrinos. In principle, such a difference in PNC potentials affects PNC effects in atoms and may be used to determine what the nature is of neutrinos. However, this difference is significant at $r \gtrsim \hbar/m_\nu c$. At small distance, where the PNC potential gives a dominating contribution to the matrix elements, the difference is negligible. Instead, one may think about some larger distance macroscopic effects produced by the neutrino PNC potential. Such experiments have been done for the parity-conserving potentials—see Refs. [5–9]. Recently, the measurement was done for a PNC potential due to a hypothetical Z' boson with the interaction range from 3 mm to 0.1 km [43]. We may reinterpret the results for the Eq. (11) potential. However, rapid decay $\sim1/r^5$ indicates that the corresponding PNC effect due to neutrino potential Eq. (11) will be very small at such a distance. The corresponding limit on the effective interaction constant is very weak, $G_{\rm eff}^2/G^2 \lesssim 10^{33}$. A measurement at a much smaller distance is needed.

[1] R. P. Feynman, *Feynman Lectures on Gravitation* (Addison-Wesley, Reading, MA, 1996).

[2] G. Feinberg and J. Sucher, Phys. Rev. **166**, 1638 (1968).

[3] G. Feinberg, J. Sucher, and C.-K. Au, Phys. Rep. **180**, 83 (1989).

[4] S. D. H. Hsu and P. Sikivie, Phys. Rev. D **49**, 4951 (1994).

[5] D. J. Kapner, T. S. Cook, E. G. Adelberger, J. H. Gundlach, B. R. Heckel, C. D. Hoyle, and H. E. Swanson, Phys. Rev. Lett. **98**, 021101 (2007).

[6] E. G. Adelberger, B. R. Heckel, S. Hoedl, C. D. Hoyle, D. J. Kapner, and A. Upadhye, Phys. Rev. Lett. **98**, 131104 (2007).

[7] Y.-J. Chen, W. K. Tham, D. E. Krause, D. Lopez, E. Fischbach, and R. S. Decca, Phys. Rev. Lett. **116**, 221102 (2016).

[8] G. Vasilakis, J. M. Brown, T. W. Kornack, and M. V. Romalis, Phys. Rev. Lett. **103**, 261801 (2009).

[9] W. A. Terrano, E. G. Adelberger, J. G. Lee, and B. R. Heckel, Phys. Rev. Lett. **115**, 201801 (2015).

[10] Y. V. Stadnik, Phys. Rev. Lett. **120**, 223202 (2018).

[11] M. Ghosh, Y. Grossman, and W. Tangarife, Phys. Rev. D **101**, 116006 (2020).

[12] V. V. Flambaum and E. V. Shuryak, Phys. Rev. C **76**, 065206 (2007).

[13] C. S. Wood, S. C. Bennett, D. Cho, B. P. Masterson, J. L. Roberst, C. E. Tanner, and C. E. Wieman, Science **275**, 1759 (1997).

[14] V. A. Dzuba, V. V. Flambaum, and O. P. Suskov, Phys. Lett. A **141**, 147 (1989).

[15] V. A. Dzuba, V. V. Flambaum, and J. S. M. Ginges, Phys. Rev. D **66**, 076013 (2002).

[16] S. A. Blundell, W. R. Johnson, and J. Sapirstein, Phys. Rev. Lett. **65**, 1411 (1990).

[17] S. A. Blundell, J. Sapirstein, and W. R. Johnson, Phys. Rev. D **45**, 1602 (1992).

[18] V. V. Flambaum and J. S. M. Ginges, Phys. Rev. A **72**, 052115 (2005).

[19] S. G. Porsev, K. Beloy, and A. Derevianko, Phys. Rev. Lett. **102**, 181601 (2009).

[20] S. G. Porsev, K. Beloy, and A. Derevianko, Phys. Rev. D **82**, 036008 (2010).

[21] V. A. Dzuba, J. C. Berengut, V. V. Flambaum, and B. Roberts, Phys. Rev. Lett. **109**, 203003 (2012).

[22] A. Damitz, G. Toh, E. Putney, C. E. Tanner, and D. S. Elliott, Phys. Rev. A **99**, 062510 (2019).

[23] G. Toh, A. Damitz, N. Glotzbach, J. Quirk, I. C. Stevenson, J. Choi, M. S. Safronova, and D. S. Elliott, Phys. Rev. A **99**, 032504 (2019).

[24] J. A. Quirk, A. Damitz, C. E. Tanner, and D. S. Elliott, Phys. Rev. A **105**, 022819 (2022).

[25] H. B. Tran Tan, D. Xiao, and A. Derevianko, Phys. Rev. A **105**, 022803 (2022).

[26] V. A. Dzuba, V. V. Flambaum, and I. B. Khriplovich, Z. Phys. D **1**, 243 (1986).

[27] B. A. Brown, A. Derevianko, and V. V. Flambaum, Phys. Rev. C **79**, 035501 (2009).

[28] A. V. Viatkina, D. Antypas, M. G. Kozlov, D. Budker, and V. V. Flambaum, Phys. Rev. C **100**, 034318 (2019).

[29] D. Antypas, A. Fabricant, J. E. Stalnaker, K. Tsigutkin, V. V. Flambaum, and D. Budker, Nat. Phys. **15**, 120 (2019).

[30] B. M. Roberts, V. A. Dzuba, and V. V. Flambaum, Annu. Rev. Nucl. Part. Sci. **65**, 63 (2015).

[31] M. S. Safronova, D. Budker, D. DeMille, Derek F. Jackson Kimball, A. Derevianko, and C. W. Clark, Rev. Mod. Phys. **90**, 025008 (2018).

[32] W. J. Marciano and A. Sirlin, Phys. Rev. D **27**, 552 (1983).

[33] V. V. Flambaum, Phys. Rev. A **45**, 6174 (1992).

[34] M. Tanabashi, K. Hagiwara, K. Hikasa, K. Nakamura, Y. Sumino, F. Takahashi, J. Tanaka, K. Agashe, G. Aielli, C. Amsler *et al.* (Particle Data Group), Phys. Rev. D **98**, 030001 (2018).

[35] V. A. Dzuba, V. V. Flambaum, P. G. Silvestrov, and O. P. Suskov, J. Phys. B **20**, 1399 (1987).

[36] V. N. Novikov, O. P. Sushkov, V. V. Flambaum, and I. Khriplovich, JETP **46**, 420 (1977).

[37] V. V. Flambaum and I. Khriplovich, JETP **52**, 835 (1980).

[38] V. V. Flambaum, I. Khriplovich, and O. P. Sushkov, Phys. Lett. B **146**, 367 (1984).

[39] V. V. Flambaum and I. Khriplovich, JETP **62**, 872 (1985).

[40] X.-J. Xu and B. Yu, J. High Energy Phys. 02 (2022) 008.

[41] J. A. Grifols, E. Masso, and R. Toldra, Phys. Lett. B **389**, 563 (1996).

[42] S. G. Karshenboim and V. A. Shelyuto, Eur. Phys. J. D **75**, 49 (2021).

[43] Y. Wang, Y. Huang, C. Guo, M. Jiang, X. Kang, H. Su, Y. Qin, W. Ji, D. Hu, X. Peng *et al.*, arXiv:2205.07222.